Extended Depth of Field Iris Recognition with Correlation Filters

Naresh Boddeti and B. V. K. Vijaya Kumar

Abstract— Iris recognition can offer high-accuracy person recognition, particularly when the acquired iris image is well-focused. However, some practical applications require that the iris recognition system perform well even when the eyes are not in the focal plane of the camera lens. Therefore, iris recognition using camera systems with a large depth of field is very desirable. One approach to achieve extended depth of field is to use a wavefront coding system as proposed by Dowski and Cathey [1] which uses a cubic phase modulation mask whose effect is a linear operation. The conventional approach is to restore the iris images from the camera outputs and then apply iris recognition algorithms to the restored iris images. Some correlation filters are invariant to linear operations and should maintain their recognition performance even when the training and testing images are the unrestored (i.e., blurred due to wavefront coding) images produced by the extended depth of field imaging system. In this work we investigate the recognition performance of correlation filters and compare it with the popular iriscode method when the input images are unrestored images produced by the wavefront coding imaging system. We present results of simulations done with more than 1000 such unrestored wavefront coded iris images taken from the ICE database.

I. INTRODUCTION

Sharply focused iris images are necessary to be able to capture the rich texture detail of the iris which is where the discriminative information lies. The performance of an iris recognition system depends greatly on how well the iris acquisition system captures this texture detail which generally requires the iris to be within the focus volume of the acquisition system. Hence conventional iris image acquisition systems require user co-operation to a large extent in positioning their head so that the eyes are located within the focus volume of the imaging systems to get a sharply focused image. For greater flexibility and robustness, we would want the iris aquisition system to have a greater depth of field.

The traditional solution to increased depth of focus (also called depth of field) is to increase the f-number of the lens which translates to using a smaller aperture. However, doing so would increase the exposure time to allow sufficient light to enter through the smaller aperture. Increased exposure time introduces motion blur since it would be unrealistic to expect the eyes to be perfectly still for the duration of the exposure. Moreover, a smaller aperture also decreases the effective resolution of the camera system due to diffraction.
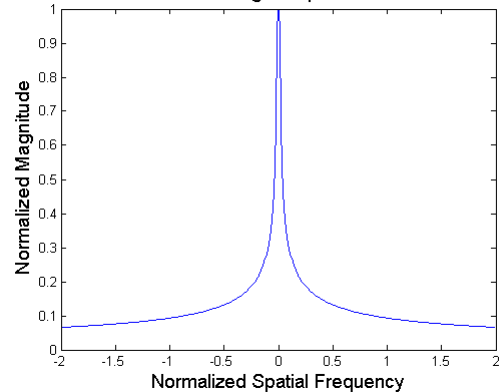
The authors are with the Department of Electrical and Computer Engineering and CyLab, Carnegie Mellon University, Pittsburgh, PA 15213, USA {vboddeti,kumar}@ece.cmu.edu
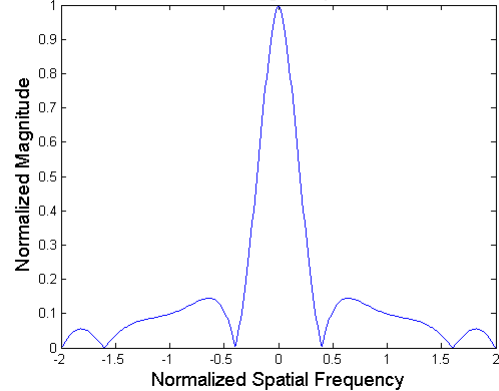
(a) MTF with no wavefront coding

(b) MTF with wavefront coding

Fig. 1: Mis-focus MTF

One way to achieve extended depth of focus without sacrificing aperture size is to take advantage of computational imaging which combines optics with digital signal processing. To extend the depth of focus of an imaging system, Dowski and Cathey [1][2] proposed the use of a phase mask. The idea is to use phase modulation to encode the depth information thereby increasing focus invariance along the axis of the lens. Under mis-focus, unlike the Modulation Transfer Function (MTF) of a conventional optical system, the MTF of a system with a cubic phase mask has no nulls (See Fig. 1). Avoiding MTF nulls is attractive since the total entropy is conserved and there is no loss of information. This means that, at least in theory we can recover the original information and acheive greater depth of focus at the same time. Many correlation filters (such as the minimum average correlation energy (MACE) filter) can compensate for any

information preserving linear operation as long as the same linear operation is applied on both the gallery and the probe images. So this makes it particularly attractive to use correlation filters for iris recognition on wavefront-coded imagery. Unlike other iris recognition approaches, correlation filters may allow us to use raw (or unrestored) image outputs from the camera for iris recognition and thus avoid the complexity and hardware associated with processing the camera outputs to obtain restored iris images. In this paper, we will refer to two types of iris images: conventional images are those obtained without any wavefront coding and wavefront-coded images refer to the raw output images (i.e., without restoring the wavefront-coded images as is commonly done) from an imaging system employing wavefront coding.

This paper is organised as follows. We first describe the pre-processing done to the iris images followed by the feature extraction employed. Next we describe the two kinds of matching that we compare, namely iriscode and correlation filters. Then we describe how we simulate the iris image data and discuss the recognition results on this simulated data. Finally we conclude with some observations and analysis of our results.

II. PRE-PROCESSING

Before we extract texture features or perform matching we need to pre-process the iris images. This involves segmentation of the iris, normalization of the iris to be able to compare irises of different sizes and removing eyelashes or any other specularities.

A. Segmentation

The performance of iris recognition systems is greatly dependent on the ability to isolate the iris from the other parts of the eye like eyelids, eyelashes etc. This is generally done through some variants of edge detection. Since the blurring introduced by the image being out of focus smudges the edge information to the point of there not being a discernible edge, iris segmentation becomes a challenging task. To overcome this problem to an extent, we use a region based active contour segmentation [3] since it is more robust to blurring than an edge based active contour. Fig.s 2 and 3 show some of our segmentation results on iris images (obtained via the simulations, to be explained in Section V) at various distances from the focal plane of the camera system. Note that at 0 cm, conventional iris images exhibit more detail than wavefront-coded images. However, over the distance ranges shown, conventional iris images exhibit more variability than wavefront-coded iris images.

B. Normalization

Once the iris boundaries have been found, we map the iris pattern into the polar domain as is popularly done. This has two effects.

1) Normalizes different irises to the same size thus allowing for proper matching.
2) Any rotation of the iris manifests as a linear shift in the polar domain which can be handled easily by both correlation filters and iriscode (via circular shifts).
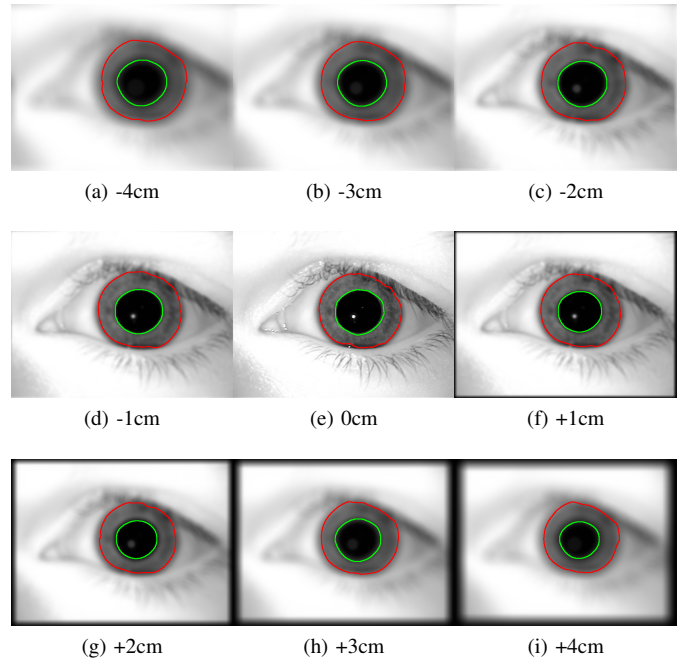

(a) -4cm	(b) -3cm	(c) -2cm
(d) -1cm	(e) 0cm	(f) +1cm
(g) +2cm	(h) +3cm	(i) +4cm

Fig. 2: Examples of iris segmentation on conventional images

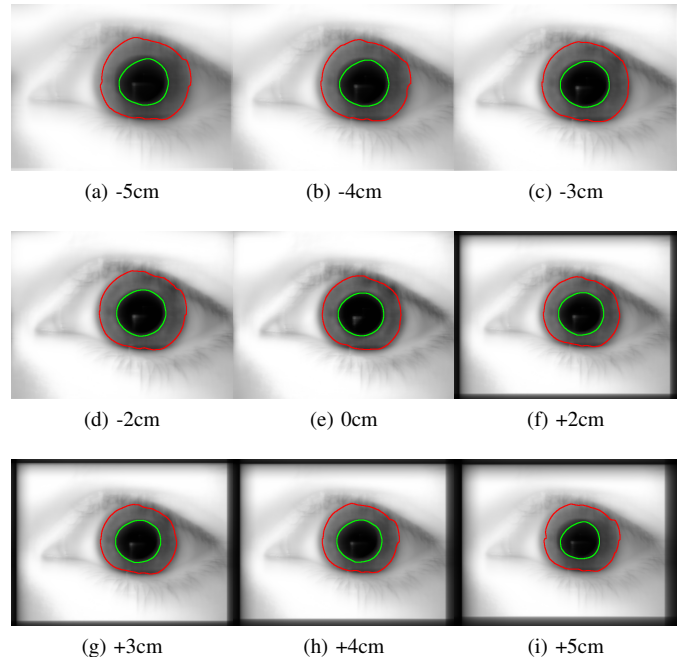| (a) -5cm | (b) -4cm | (c) -3cm |
| (d) -2cm | (e) 0cm | (f) +2cm |
| (g) +3cm | (h) +4cm | (i) +5cm |

Fig. 3: Examples of iris segmentation on wavefront-coded images

III. FEATURE EXTRACTION

Gabor filters tuned with the right parameters have been found to be the most discriminative bandpass filters for iris image feature extraction among a variety of wavelet candidates [4]. A Gabor filter is a modulated Gaussian envelope and is given by

$$g(\rho,\phi)=\exp\left[-\frac{1}{2}\left(\frac{\rho^2}{\sigma_\rho^2}+\frac{\phi^2}{\sigma_\phi^2}\right)-j\rho(\omega\sin\theta)-j\phi(\omega\cos\theta)\right]$$
$$\tag{1}$$

in the polar domain (ρ,ϕ) where the filter is applied to the iris pattern. Here θ denotes the wavelet orientation, σ_ρ and σ_ϕ denote the wavelet size in radial and angular directions, respectively and ω denotes the modulation frequency of the wavelet. By varying these parameters, the filters can be tuned to extract features at different scales, rotations, frequencies and translations. We use a set of these differently localized Gabor filters as our feature extraction filter bank. The filter bank has 2 scales and 4 orientations for a total of 8 channels in our experiments. We also divide the unwrapped iris into multiple patches when using correlation filters for matching and the projections of these patches on the Gabor bases are our features. We finally combine the recognition cues (correlation peak sharpness metrics) of each patch to come up with a final match score. Another point to note is that the band pass filters we use for feature extraction have been optimised on in-focus conventional iris images and we use the same Gabor filters throughout our experiments.

IV. MATCHING

One of the goals of this work is to compare the performance of the popular iriscode method [5][6][7] of matching with correlation filter based matching.

A. Iriscode

The phase of the complex Gabor wavelet projections obtained as explained in the previous section are quantized to 2 bits by mapping the phase to one of the four quadrants in the complex plane. All the bits obtained this way constitute an iriscode. Any two irises are compared by matching their respective iriscodes. The matching is done by computing the Hamming distance between the 2 binary iriscodes. There are also corresponding mask bits to identify which bits in the iriscode to use for matching. The mask bits are set to either 1 or 0 depending on whether the corresponding iriscode bits are used or not used (e.g., due to eyelid occlusions) for matching. When matching 2 iriscodes A and B with respective masks m_A and m_B the dissimilarity d is defined as,

$$d=\frac{||(A\oplus B)\cap m_A\cap m_B||}{||m_A\cap m_B||}\tag{2}$$

where $\oplus$ denotes an XOR operation and $||\ ||$ denotes the weight (i.e., the number of nonzero elements) of the binary pattern. Rotation of the eye is compensated for by matching the the iriscodes at different relative shifts along the angular axis and taking the minimum Hamming distance value.

B. Correlation Filters

A correlation filter is a template that is specifically designed to recognize a particular pattern class represented by a set of reference patterns [8][9]. A given query pattern is matched against this template by performing a cross-correlation. To make this efficient, the cross-correlation is
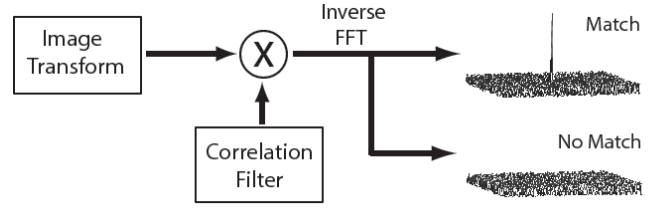

Fig. 4: Application of correlation filter to an input image

performed in the frequency domain taking advantage of the Fast Fourier Transform (FFT).

$$C(x,y)=FT^{-1}\{FT\{I(x,y)\}\cdot F^*(u,v)\}\tag{3}$$

where $I(x,y)$ is a query pattern and $F(u,v)$ is the frequency domain representation of the correlation filter.

The resulting cross-correlation output $C(x,y)$ should contain a sharp peak if the query is authentic and no such peak if it is an impostor as shown in Fig. 4.

The principal advantages of using correlation filters are:

1) Generation of the whole correlation plane in one shot.
2) Graceful performance degradation in the presence of noise or occlusions.
3) Can be designed to tolerate a variety of within-class variations.
4) Closed form solution for the filters.

To quantify the degree of sharpness of the correlation peak we use the peak-to-correlation (PCE) ratio defined as:

$$PCE=\frac{peak-\mu}{\sigma}\tag{4}$$

where μ and σ are the mean and standard deviation of the correlation plane respectively.

There are a variety of advanced correlation filters to choose from [10]. Among these MACE [11] filter and Optimal Tradeoff Synthetic Discriminant Function (OTSDF) filter [12] (a more general form of MACE filter) have been found to perform well when applied to biometric recognition problems [13][14][15].

In this work we use the OTSDF filter which provides an optimal trade-off between the Average Correlation Energy (ACE) and the Output Noise Variance (ONV). The ACE is the energy in the correlation plane averaged over the training images minimizing which suppresses the side lobes resulting in sharp correlation peaks. Minimizing ONV improves the filter's tolerance towards noise. Formulating this in a Lagrangian framework gives us a closed form solution for the optimal trade-off filter.

Fusion OTSDF

Since our iris patterns are represented as multi-channel features we can design one filter for each channel and combine the resulting correlation plane outputs. However one can do better by jointly optimizing the K filters [16], such

filters are referred to as "fusion correlation filters". This leads to

$$H = A^{-1}X(X^+A^{-1}X)^{-1}u \quad (5)$$

where H is the frequncy domain representation of the correlation filter, $A = \alpha S + (1-\alpha)\bar{P}$ and S is the cross-power spectral density matrix of the noise in the channels and $\bar{P}$ is the mean cross-power spectral density between the different feature channels. See Appendix A for more details on fusion OTSDF design and use.

V. SIMULATIONS

A. Database

In this work we used a subset of the Iris Challenge Evaluation (ICE) dataset. Sixty one users were manually selected such that most of the images of the user are either in focus or close to being in focus. We avoided classes with only one image in the database and classes with heavy eyelash occlusions. In total our evaluation was done on 1061 images. This was done to ensure that the evaluation is closer to a practical situation where the exact amount of blurring is unknown and other factors like poor segmentation affect recognition performance. The chosen images have been used to simulate both the wavefront-coded images and the conventional out of focus images. Fig. 5 and 6 show some samples.
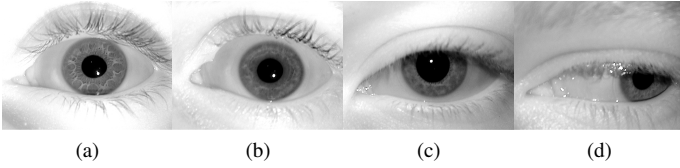

(a)　　　　(b)　　　　(c)　　　　(d)

Fig. 5: Examples of images used for evaluation
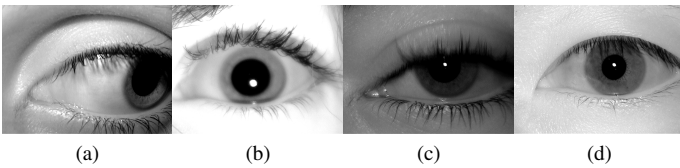

(a)　　　　(b)　　　　(c)　　　　(d)

Fig. 6: Examples of images avoided for evaluation. (a) too close to boundary and would get worse when simulating iris images nearer to camera (b) badly out of focus (c) very low constrast between pupil and iris along with eyelid shadow (d) eyelashes on the iris

B. Simulation Methodology

The simulation was done by convolving the in-focus images with the point spread function (PSF) of both a normal and wavefront-coded imaging system. This is given by

$$g = h * f + \eta \quad (6)$$

where g is the blurred and noisy output image, h is the PSF of the imaging system, f is the ground truth image and η is the poisson noise which following the common model [17] is given by

$$\eta = \sqrt{h * f}\eta_1 + \sigma\eta_2 \quad (7)$$

where η_1 and η_2 are N(0,1) random variables and σ is the standard deviation of the image-independent noise.

The PSF model used for the two types of imagery is as given in (8) and (10).

Conventional System:

$$h = |FT\{P(x,y)e^{(i\psi(x^2+y^2))}\}|^2 \quad (8)$$

where $P(x,y)$ is 1 inside the pupil and 0 outside and the misfocus parameter ψ is given by

$$\psi = \frac{\pi L^2}{4\lambda}\left(\frac{1}{f} - \frac{1}{d_o} - \frac{1}{d_i}\right) \quad (9)$$

where L is the pupil diameter, λ is the wavelength of light used, f is the focal length of the lens, d_o is the object distance from the first principal plane of the lens and d_i is the distance between the second principal plane of the lens and the image plane.

Wavefront Coding System:

$$h = |FT\{P(x,y)e^{(i(\psi(x^2+y^2)+\phi(x,y)))}\}|^2 \quad (10)$$

where $\phi(x,y)$ is the phase function of the mask. In this work we used a cubic phase mask $\phi = \beta(x^3 + y^3)$ with β being the strength of the mask. One could also use other phase functions but for this initial evaluation we chose the cubic phase function for consistency with earlier work. The camera parameters have been chosen based on published literature [18][19][20].

C. Sample Images

The images were simulated to cover a distance of 10cm in either direction from the focal plane with a step size of 1cm. Fig. 7 show some sample iris images at various distances.

VI. RESULTS

In this section we present the results obtained using iriscode (our baseline) as well as correlation filters based iris pattern matching. All the experiments were carried out on unrestored images because we want to study the feasibility of avoiding the reconstruction step in wavefront-coded iris imaging.

A. Experiments

We conducted two kinds of experiments corresponding to slightly different scenarios.

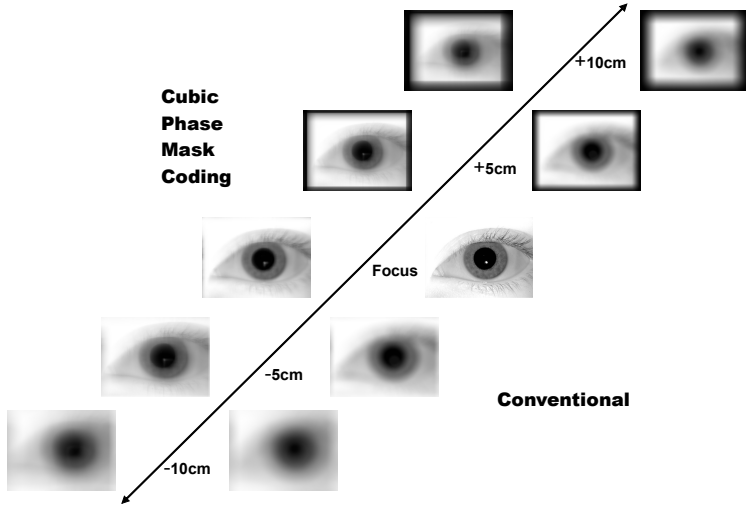1) Train using images in-focus (both conventional and wavefront-coded) and test on images at various distances.

Fig. 7: Sample Simulated images of both conventional and cubic phase mask optical system

2) Train using sample images at different distances (can be obtained from the in-focus image by simulation) and test on images at various distances. In this case a single fusion OTSDF filter is built just like in the first scenario except that we use images at other distances also for training. For iriscodes this is done by matching the probe iriscode to template iriscodes at different distances and taking the minimum Hamming distance as the match score.

In the second scenario the templates are trained using images from different distances, hence the algorithms are expected to perform better than the first scenario where the template sees only images in focus with and without the phase mask. In our experiments we use images at distances of -2cm to +2cm only from the focal plane in the template. We do not use images at larger distances in our template because poor segmentation at greater distances may affect the overall filter design. However, there may not be such a penalty in matching iriscodes. The matching complexity with correlation filters would not change in the second scenario because the matching is done with only one template while the matching complexity increases linearly for iriscode. For proper comparison we use the same training sets for both iriscode and correlation filter based matching.
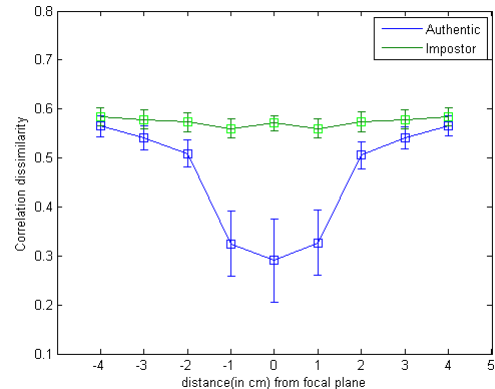
B. Results

We look at the impostor and authentic score statistics (mean and standard deviation of match score plotted as small squares and vertical bars, respectively) to determine the improvement in the imaging distance obtained compared to the conventional iris imaging system.

Scenario 1: Fig. 8 and 9 show the results of conventional and cubic phase mask coded optical system, respectively. Defining the operational range as the distance upto which the error bars of the authentic and impostor scores do not overlap, we compare the approximate operational range of the iris recognition system both with and without the phase mask in Table I. We also compare the performance of the two different matching techniques (See Table II). We see that both iriscode and correlation filters significantly increase the operational distance of the recognition system. Correlation filters, due to the added advantage of being invariant to linear operations perform slightly better than iriscode as reflected in the larger operational range. Tables III and IV compare the recognition performance in both the conventional scenario and the wavefront coded scenario. Even though the increase in the depth of field of correlation filters over iriscode may not appear to be large, the recognition performance of correlation filters is better than iriscode over the range of the depth of field when wavefront coded imagery is used.
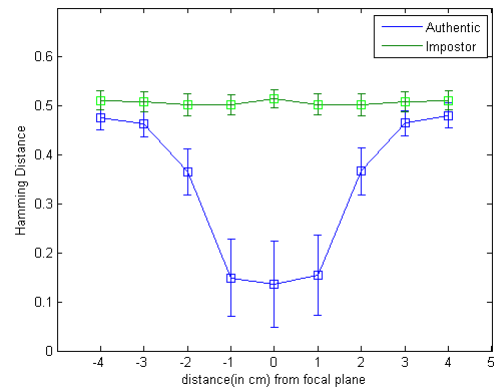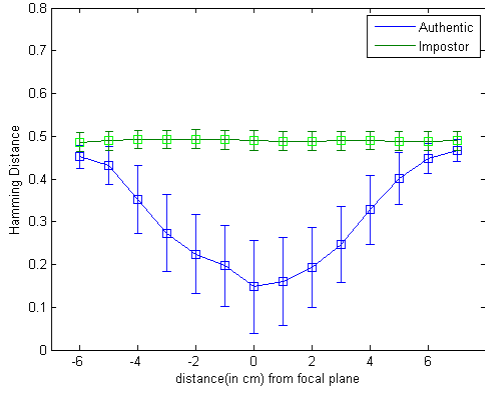

(a) Iriscode on conventional images

(b) Correlation Filters on conventional images

Fig. 8: Results of both Iriscode and Correlation Filters for the conventional optical system in the first scenario.

Scenario 2: Fig. 10 and 11 show the results of conventional and cubic phase mask coded optical system, respectively. Tables V and VI compare the performance of both iriscode and correlation filters on both conventional and wavefront-coded imagery. We can see a clear increase in the

(a) Iriscode on unrestored wavefront-coded images

(b) Correlation Filters on unrestored wavefront-coded images

Fig. 9: Results of both Iriscode and Correlation Filters for the coded optical system in the first scenario.

TABLE I: Operational Range Comparison (Scenario I)

Iriscode			
Data Type	Distance (in cm)		Operational Range (in cm)
Conventional	-2.9	2.9	∼5.8
Wavefront-Coded	-4.8	5.3	∼10.1
Correlation Filters			
Data Type	Distance (in cm)		Operational Range (in cm)
Conventional	-2.7	2.7	∼5.4
Wavefront-Coded	-6.1	6.5	∼12.6

TABLE II: Comaprison of Operational Range Improvement

Operational Range	Conventional (in cm)	Wavefront (in cm)	Improvement
Iriscode	5.8	10.1	∼1.75
Correlation Filters	5.4	12.6	∼2.34

operational range in the case of iriscode. While this is not so apparent in the case of correlation filters, we notice an increase in the separation between the mean authentic and impostor scores for distances whose samples were used for training the filter. This suggests that including samples from other distances might further help increase the range. We also notice that both correlation filters and iriscode perform

TABLE III: Recognition Performance Conventional FRR at FAR in percentage

Distance (in cm)	Iriscode (1.0 and 0.1)		CF (1.0 and 0.1)	
-4	76.2	93.0	88.3	96.8
-3	69.2	93.0	64.8	82.6
-2	3.30	11.2	27.5	49.4
-1	0.56	0.67	0.56	1.00
0	0.44	0.67	0.60	0.90
1	1.10	1.30	0.70	1.10
2	5.00	15.6	23.2	47.5
3	68.7	93.6	64.7	82.7
4	78.2	93.7	88.6	97.3

TABLE IV: Recognition Performance Wavefront Coded FRR at FAR in percentage

Distance (in cm)	Iriscode (1.0 and 0.1)		CF (1.0 and 0.1)	
-6	72.8	91.6	44.5	66.3
-5	37.9	59.7	8.90	15.3
-4	8.20	15.0	2.90	5.20
-3	3.50	6.80	1.60	2.80
-2	1.60	2.60	1.10	1.70
-1	1.50	2.30	0.68	1.20
0	1.10	1.30	0.56	1.10
1	0.90	1.70	0.68	1.20
2	1.70	2.10	1.20	1.60
3	3.50	3.90	1.40	2.80
4	7.50	93.7	2.30	4.80
5	23.3	38.5	5.90	10.5
6	62.1	82.2	24.4	42.7
7	87.4	97.3	69.2	84.8

better at distances slightly away from the focal plane than when the iris is in focus. This is due to the fact that small variations affect the appearance of the in-focus images more than they affect the slightly blurred images. When the images are slightly blurred all the extranous high frequency effects like noise or other unwanted variations are smoothed out even while preserving the underlying iris texture pattern. This helps improve tolerance to slight variations leading to better performance. Such an effect was also observed in fingerprint recognition with correlation filters [21] where higher resolution did not always yield better recognition accuracy. However, as the blurring increases, the recognition performance decreases as the texture detail starts disappearing.

We also observed that a major challenge to increasing the operational range of iris recognition systems comes from iris segmentation which becomes increasingly difficult with

TABLE V: Operational Range Comparison (Scenario II)

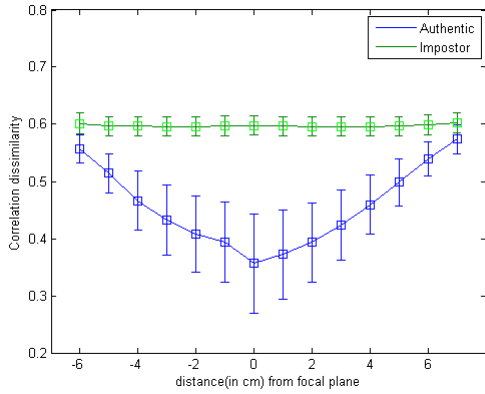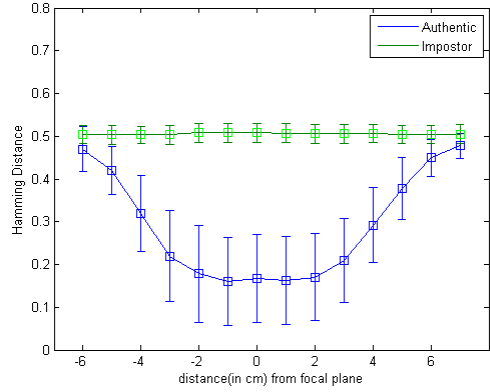| Iriscode			
Data Type	Distance (in cm)		Operational Range (in cm)
Conventional	-4.0	3.8	∼7.8
Wavefront-Coded	-5.5	6.0	∼11.5
Correlation Filters			
Data Type	Distance (in cm)		Operational Range (in cm)
Conventional	-3.6	3.5	∼7.1
Wavefront-Coded	-5.9	6.3	∼12.2
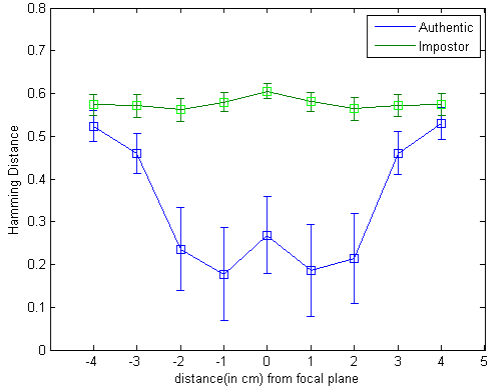
(a) Iriscode on conventional images
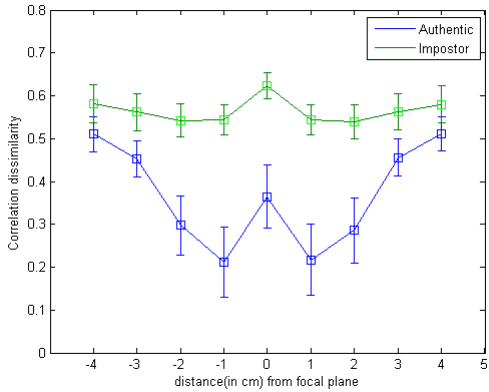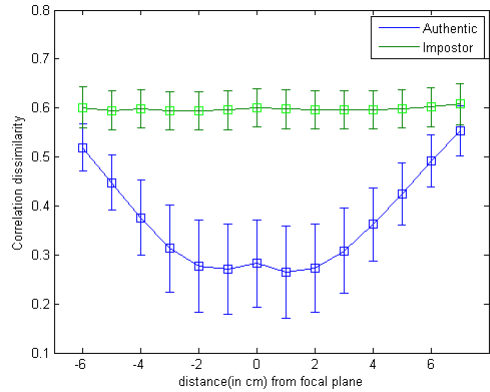
(b) Correlation Filters on conventional images

Fig. 10: Results of both Iriscode and Correlation Filters for the conventional optical system in the second scenario.

(a) Iriscode on unrestored wavefront-coded images

(b) Correlation Filters on unrestored wavefront-coded images

Fig. 11: Results of both Iriscode and Correlation Filters for the coded optical system in the second scenario.

TABLE VI: Comparison of Operational Range Improvement

Operational Range	Conventional (in cm)	Wavefront (in cm)	Improvement
Iriscode	7.8	11.5	∼1.5
Correlation Filters	7.1	12.2	∼1.7

increasing distance from the focal plane. Improving the segmentation would enable us to use the full power of the matching techniques to get greater depth of focus without modifying the existing matching techniques. In other words we believe that segmentation is the key to increasing the depth of field using the phase mask and without doing image restoration.

VII. CONCLUSIONS AND FUTURE WORKS

Iris recognition technology can acheive very high matching accuracy but still requires substantial user co-operation. To ease this requirement on the user, we require that the operational range of the iris acquisition system be larger than what it is today. Wavefront coding offers a solution to acheive this, but there have not been any large scale tests to quantify and confirm the increase in the depth of field that can be acheived. In this work we address this problem by using more than 1000 images for evaluation without restoring the blurred

images thereby saving the additional computations required for image restoration. Our results also show that correlation filters are better suited to handle out of focus images better than a simple Hamming distance based matching because of the built-in tolerance of correlation filters to noise and entropy-preserving linear operations.

We plan to conduct a more thorough investigation of the application of wavefront coding to iris recognition. This would include improved iris segmentation taking into account the kind of blurring introduced by the phase mask, finding optimum bandpass filters for feature extraction across different distances and phase functions and phase function optimisation with respect to recognition accuracy.

VIII. ACKNOWLEDGMENTS

APPENDIX A: Details of Fusion OTSDF

Let a pattern be represented by K feature channels. Taking the discrete fourier transform of each channel and arranging the DFT coefficients and correlation filter values into a vector

we have:

$$\mathbf{x}_i \triangleq \left[\begin{array}{c} M \\ \times \\ 1 \end{array}\right] \begin{array}{l} \text{Image DFT} \\ \text{coefficients,} \\ \text{channel } i \end{array} \qquad \mathbf{h}_i \triangleq \left[\begin{array}{c} M \\ \times \\ 1 \end{array}\right] \begin{array}{l} \text{Filter} \\ \text{coefficients,} \\ \text{channel } i \end{array} \tag{11}$$

Vector $\mathbf{x}$ is formed by appending all the feature channels for a training image. We do the same for the correlation filter to get:

$$\mathbf{x} \triangleq \left[\begin{array}{c} \mathbf{x}_1 \\ \mathbf{x}_2 \\ \vdots \\ \mathbf{x}_K \end{array}\right] \qquad \mathbf{h} \triangleq \left[\begin{array}{c} \mathbf{h}_1 \\ \mathbf{h}_2 \\ \vdots \\ \mathbf{h}_K \end{array}\right] \tag{12}$$

We now define $\mathbf{X}$ as a matrix containing the jth training vector $\mathbf{x}^{(j)}$ in the jth column:

$$\mathbf{X} \triangleq \left[\begin{array}{cccc} \mathbf{x}_1^{(1)} & \mathbf{x}_1^{(2)} & \cdots & \mathbf{x}_1^{(N)} \\ \mathbf{x}_2^{(1)} & \mathbf{x}_2^{(2)} & \cdots & \mathbf{x}_2^{(N)} \\ \vdots & \vdots & & \vdots \\ \mathbf{x}_K^{(1)} & \mathbf{x}_K^{(2)} & \cdots & \mathbf{x}_K^{(N)} \end{array}\right] \tag{13}$$

Average Correlation Energy (ACE): The correlation plane energy by Parseval's is defined as:

$$E = \mathbf{h}^+\mathbf{Ph}$$

$$= \left[\begin{array}{c} \mathbf{h}_1 \\ \mathbf{h}_2 \\ \vdots \\ \mathbf{h}_K \end{array}\right]^+ \left[\begin{array}{cccc} \mathbf{x}_1^*\mathbf{x}_1 & \mathbf{x}_1^*\mathbf{x}_2 & \cdots & \mathbf{x}_1^*\mathbf{x}_K \\ \mathbf{x}_2^*\mathbf{x}_1 & \mathbf{x}_2^*\mathbf{x}_2 & \cdots & \mathbf{x}_2^*\mathbf{x}_K \\ \vdots & \vdots & & \vdots \\ \mathbf{x}_K^*\mathbf{x}_1 & \mathbf{x}_K^*\mathbf{x}_2 & \cdots & \mathbf{x}_K^*\mathbf{x}_K \end{array}\right] \left[\begin{array}{c} \mathbf{h}_1 \\ \mathbf{h}_2 \\ \vdots \\ \mathbf{h}_K \end{array}\right] \tag{14}$$

Averaging over all the training data we have the Average Correlation Energy defined as:

$$\text{ACE} = \mathbf{h}^+\bar{\mathbf{P}}\mathbf{h} \tag{15}$$

$$= \left[\begin{array}{c} \mathbf{h}_1 \\ \mathbf{h}_2 \\ \vdots \\ \mathbf{h}_K \end{array}\right]^+ \left[\begin{array}{ccc} \frac{1}{N}\sum_i \mathbf{x}_1^{(i)*}\mathbf{x}_1^{(i)} & \cdots & \frac{1}{N}\sum_i \mathbf{x}_1^{(i)*}\mathbf{x}_K^{(i)} \\ \frac{1}{N}\sum_i \mathbf{x}_2^{(i)*}\mathbf{x}_1^{(i)} & \cdots & \frac{1}{N}\sum_i \mathbf{x}_2^{(i)*}\mathbf{x}_K^{(i)} \\ \vdots & & \vdots \\ \frac{1}{N}\sum_i \mathbf{x}_K^{(i)*}\mathbf{x}_1^{(i)} & \cdots & \frac{1}{N}\sum_i \mathbf{x}_K^{(i)*}\mathbf{x}_K^{(i)} \end{array}\right] \left[\begin{array}{c} \mathbf{h}_1 \\ \mathbf{h}_2 \\ \vdots \\ \mathbf{h}_K \end{array}\right]$$

Output Noise Variance (ONV): Let S_{ab} contain the cross-power spectral density between noise in channel a and channel b. Now ONV is defined as:

$$\text{ONV} = \mathbf{h}^+\mathbf{Sh} \tag{16}$$

$$= \left[\begin{array}{c} \mathbf{h}_1 \\ \mathbf{h}_2 \\ \vdots \\ \mathbf{H}_K \end{array}\right]^+ \left[\begin{array}{cccc} \mathbf{S}_{11} & \mathbf{S}_{12} & \cdots & \mathbf{S}_{1K} \\ \mathbf{S}_{21} & \mathbf{S}_{22} & \cdots & \mathbf{S}_{2K} \\ \vdots & \vdots & & \vdots \\ \mathbf{S}_{K1} & \mathbf{S}_{K2} & \cdots & \mathbf{S}_{KK} \end{array}\right] \left[\begin{array}{c} \mathbf{h}_1 \\ \mathbf{h}_2 \\ \vdots \\ \mathbf{h}_K \end{array}\right]$$

The Lagrangian framework of the optimal tradoff between the ACE and ONV gives:

$$\mathbf{h} = \mathbf{A}^{-1}\mathbf{X}(\mathbf{X}^+\mathbf{A}^{-1}\mathbf{X})^{-1}\mathbf{u} \tag{17}$$

where $\mathbf{h}$ is the frequncy domain representation of the correlation filter and $\mathbf{A} = \alpha\mathbf{S} + (1-\alpha)\bar{\mathbf{P}}$

REFERENCES

[1] Edward R. Dowski and W. Thomas Cathey, "Extended depth of field through wave-front coding," *Applied Optics*, vol. 34, no. 11, pp.1859-1866, 1995

[2] W. Thomas Cathey and Edward R. Dowski, "New paradigm for imaging systems," *Applied Optics*, vol. 41, no. 29, pp. 6080-6092, 2002.

[3] Tony F. Chan and Luminita A. Vese, "Active Contours without Edges," *IEEE Transaction on Image Processing*, vol 10, no. 2, pp. 266-277, February 2001

[4] Jason Thronton,Marios Savvides and B.V.K Vijaya Kumar, "An Evaluation of Iris Pattern Representation," *BTAS 2007*, September 2007.

[5] John Daugman, "How Iris Recognition Works," *International Conference on Image Processing*, vol. 1, pp. 33-36, 2002

[6] John Daugman, "New Methods in Iris Recognition," *IEEE Transactions on Systems, Man, and Cybernetics*, vol. 37, no. 5, pp. 1167-1175, October 2007.

[7] John Daugman, "High confidence visual recognition of persons by a test of statistical independence," *IEEE Transactions on Pattern Analysis and Machine Intelligence*, vol. 15, no. 11, pp. 1148-1161, November 1993.

[8] C.F. Hester and D. Casasent, "Multivariant technique for multiclass pattern recognition," *Applied Optics*, vol. 19, pp. 1758-1761, 1980.

[9] B.V.K Vijaya Kumar and A. Mahalanobis, "Recent advances in composite correlation filter designs," *Asian Journal of Physics*, vol.8, no. 3, 1999.

[10] B.V.K Vijaya Kumar, "Tutorial Survey of Composite Filter Designs for Optical Correlators," *Applied Optics*, vol. 31, pp. 4773-4801, 1992.

[11] A. Mahalanobis, B.V.K Vijaya Kumar and D. Casasent, "Minimum average correlation energy filters," *Applied Optics*, vol. 26, pp. 3633-3640,1987.

[12] B.V.K. Vijaya Kumar, D.W. Carlson and A. Mahalanobis, "Optimal trade-off synthetic discriminant function filters for arbitrary devices," *Optics Letters*, vol. 19, pp. 1556-1558, 1994.

[13] B.V.K Vijaya Kumar, M. Savvides, K. Ventakaramani and C. Xie, "Spatial frequency domain image processing for biometric recognition," *Proceedings of International Conference of Image Processing*, pp. 53-56, September 2002.

[14] M. Savvides and B.V.K. Vijaya Kumar, "Efficient design of advanced correlation filters for robust distortion-tolerant face recognition," *Proceedings of IEEE Conference on Advanced Video and Signal Based Surveillance*, pp. 45-52, July 2003.

[15] J. Thronton, M. Savvides and B.V.K. Vijaya Kumar, "Robust iris recognition using advanced correlation techniques," *Proceedings of International Conference on Image Analysis and Recognition*, pp. 1098-1105, September 2005.

[16] A. Mahalanobis and B.V.K. Vijaya Kumar, "Polynomial filters for higher-order correlation and multi-input information fusion," *Proceedings of Eleventh Euro-American Workshop*, June 1997.

[17] A. K. Jain, *Fundamentals of digital image processing* Information and System Sciences. Prentice-Hall International, 1989.

[18] R. Plemmons, M. Horvath, E. Leonhardth, P.Pauca, S.Prasad, S. Narayanswamy and P.E.X Silveira, "Computational Imaging Systems for Iris Recognition," *Proceedings of SPIE*, August 2004.

[19] R. Narayanswamy, G.E Johnson, P.E.X Silveira and Hans Wach, "Extending the imaging volumr for biometric iris recognition," *Applied Optics*, vol. 44, February 2005.

[20] Kelly N. Smith, V. Paul Pauca, Arun Ross, Todd Torgersen, Micheal C. King, "Extended Evaluation of Simulated Wavefront Coding Technology in Iris Recognition," *IEEE Internatiinal Conference on Biometrics:Theory, Applications and Systems(BTAS)*, September 2007

[21] K. Venkataramani and B.V.K. Vijaya Kumar, "Performance of composite correlation filters for fingerprint verification," *Optical Engineering*, vol. 43, 1820-27, 2004.